Draft: March 15, 2023
Preprint typeset using LaTeX style emulateapj v. 05/12/14

# SURF 2022 PROJECT: PRODUCING CII LUMINOSITY MAPS USING LICHEN'S MODEL AND `limlam_mocker`

Patrick Horlaville[1,2], Dongwoo Chung[1,3], Richard J. Bond[1]

*Subject headings:* cosmology: [CII] line intensity — modeling — galaxy — dark matter

## 1. INTRODUCTION

### 1.1. *Background*

The study of high redshift galaxies is increasingly important in the context of our understanding of galaxy formation and cosmology. While modern surveys still struggle to efficiently probe those populations, simulation techniques such as intensity mapping have proven to be able to infer the properties of those dear high redshift galaxies, *e.g.* intensity mapping of carbon monoxide and its ground-state transition (Li et al., 2016) (1).

Intensity mapping (IM), or line intensity mapping (LIM), is a technique that consists of probing the 3D sky (RA, Dec & $\nu_{obs}$) at low angular resolution of specific molecular lines (Bernal et al., 2022 (? )). The strength of this analysis resides in 1) its potential to probe large cosmological volume quickly and 2) its ability to probe galaxies invisible to standard galaxy surveys.

### 1.2. *Project context*

The goal of this project is to produce galaxies' CII luminosity maps using line intensity mapping. To do so, we make use of a publicly available program called `limlam_mocker` which allow to generate line intensity maps out of a specified halo catalogue and mass-luminosity function. The code allows the implementation of various models for various lines. For this project, we implemented a new model in the `limlam_mocker` code using a novel relationship developed by Liang et al. (2023) **??**.

Here we depict the novel relationship that gave rise to this analysis, the process to retrieve the CII luminosity along with preliminary CII forecast maps for the upcoming experiment CCAT-prime.

## 2. PROCESS

### 2.1. *A Novel Relationship*

(add a bit more context from the FIRE paper)

Liang et al. (2023) **??** derived a novel relationship for halos' CII luminosity :

$$\frac{L_{[\mathrm{CII}]}/L_\odot}{\mathrm{SFR}/(\mathrm{M_\odot yr^{-1}})} \propto f_{[\mathrm{CII}]}\overline{Z}_{\mathrm{gas}}t_{\mathrm{dep}}\overline{n}_{\mathrm{gas}},, \tag{1}$$

for $L_{[\mathrm{CII}]}$ the CII luminosity (in $[L_\odot]$), $f_{[\mathrm{CII}]}$ the fraction of the total gas mass that comes from HI and HII regions, $\overline{Z}_{\mathrm{gas}}$ the gas metallicity, $t_{\mathrm{dep}}$ the galaxy's gas depletion time ($t_{\mathrm{dep}} \equiv \frac{M_{\mathrm{gas}}}{\mathrm{SFR}}$) and $\overline{n}_{\mathrm{gas}}$ the statistical average of gas density.

### 2.2. *First model: $L_{[\mathrm{CII}]}$ as a function of HI mass*

By multiplying both sides by the SFR, we recover a proportionality relationship between $L_{[\mathrm{CII}]}$ and $M_{\mathrm{gas}}$ (from the definition of $t_{\mathrm{dep}}$). By estimating the HI gas to be the main contributor to $M_{\mathrm{gas}}$, we can express CII luminosity as:

$$L_{[\mathrm{CII}]} \propto M_{\mathrm{HI}}, \tag{2}$$

or, more particularly:

$$L_{[\mathrm{CII}]}/L_\odot = \alpha_{\mathrm{CII}} \times M_{\mathrm{HI}}/M_\odot, \tag{3}$$

for $\alpha_{\mathrm{CII}}$ the proportionality coefficient between $L_{[\mathrm{CII}]}$ and $M_{\mathrm{H1}}$.

Villaescua-Navarro et al. (2018) **??** provide a handy relationship between the total halo mass ($M_{\mathrm{halo}}$) and the amount of that mass that comes from HI ($M_{\mathrm{H1}}$) that is accurate in the $\sim [10^9,\, 10^{13}]\ M_\odot$ halo mass range:

$$M_{\mathrm{HI}}(M_{\mathrm{halo}}) = M_0(\frac{M_{\mathrm{halo}}}{M_{\mathrm{min}}})^\alpha exp(-(\frac{M_{\mathrm{min}}}{M_{\mathrm{halo}}})^{0.35}), \tag{4}$$

where $M_{\mathrm{min}}$ is the cutoff mass, $M_0$ is the overall normalization and $\alpha$ is a slope power index, all parameters for the fit relationship between $M_{\mathrm{halo}}$ and $M_{\mathrm{H1}}$. Those values are determined depending on the redshift of halos of interest. Here, we are looking into halos of $z \sim [5.8, 7.9]$, and given Villaescua-Navarro et al. provide these parameters for $z$ values up to 5, we use their $z = 5$ parameter values, namely $\alpha = 0.74$, $M_0 = 1.9 \times 10^9 M_\odot$ and $M_{\mathrm{min}} = 2.0 \times 10^{10} M_\odot$.

Our goal is to express halos' $L_{[\mathrm{CII}]}$ as a function of halo mass $M_{\mathrm{halo}}$. To do so, we can convert $M_{\mathrm{halo}}$ to $M_{\mathrm{HI}}$ through equation 4 to then find $L_{[\mathrm{CII}]}$ from equation 6. The only missing piece to this puzzle is to find $\alpha_{\mathrm{CII}}$.

To do so, we can find the corresponding CII luminosity to some halo's HI mass (namely $L_{[\mathrm{CII}]}{}^*$ and $M_{\mathrm{HI}}{}^*$) and divide the former by the latter, which should give $\alpha_{\mathrm{CII}}$ from equation 6. To alleviate our turmoil, we pick the HI mass & the CII luminosity that correspond to a SFR of 1 (such that $\mathrm{SFR}^* = 1\frac{\mathrm{M_\odot}}{\mathrm{yr}}$), as this $\mathrm{SFR}^*$ will allow to find both of them. The former is found through the halo mass $M_{\mathrm{halo}}$ and the latter can be found from the proportionality relationship between halos' [CII] luminosity and SFR as found by Liang et al. (2022) **??** (p.12, figure 7):

$$\frac{L_{[\mathrm{CII}]}}{L_\odot} \sim 10^7 \times \frac{\mathrm{SFR}}{M_\odot yr^{-1}}, \tag{5}$$

which gives $L_{[\mathrm{CII}]}{}^* = 10^7 L_\odot$.

[1] Canadian Institute for Theoretical Astrophysics (CITA)
[2] McGill University
[2] Dunlap Institute

${M_{\rm HI}}^*$ can be found from ${M_{\rm halo}}^*$ through equation 4, which in turn can be found from SFR$^*$ by using an SFR/$M_{\rm halo}$ model. Here we use the Behroozi et al. (2013) **??** SFR model to interpolate ${M_{\rm halo}}^*$ from SFR$^*$.

To summarize, we compute ${M_{\rm halo}}^*$ from SFR$^*$ using the Behroozi et al. (2013) **??** SFR model, out of which which we retrieve ${M_{\rm HI}}^*$ through equation 4. We then divide ${L_{\rm [CII]}}^*$ found from SFR$^*$ through equation 5 by ${M_{\rm HI}}^*$ to retrieve $\alpha_{\rm CII}$, which can then be used to compute the CII luminosity directly from HI mass, the latter being retrieved from halo mass through equation 4. We can hence find CII luminosity from halo mass.

Starting with SFR$^*$ = 1 $M_\odot$/year, we found $\alpha_{\rm CII} \sim 0.005$. Hence, the relationship derived for [CII] luminosity for this model is:

$$L_{\rm [CII]}/L_\odot = 0.005 \times M_{\rm HI}/M_\odot,, \tag{6}$$

where the prescription from halo mass to HI mass is given by equation 4.

### 2.3. *Second model: $L_{\rm [CII]}$ as a function of HI mass and metallicity*

Now that we determined the proportionality relationship between HI mass and [CII] luminosity, we integrate an additional variable to our model from equation 1, the metallicity $Z$, such that we would now like to model the [CII] signal as:

$$L_{\rm [CII]}/L_\odot = \alpha_{\rm CII} \times M_{\rm HI}/M_\odot \times Z/Z_\odot. \tag{7}$$

To retrieve halos' metallicity from their mass, we first find their stellar mass, from which we can find their metallicity through a fundamental metallicity relationship (FMR). We use the Behroozi et al. (2013) **??** prescription for stellar mass – halo mass (SMHM) relationship:

$$log_{10}(M_*(M_h)) = log_{10}(\epsilon M_1) + f(log_{10}(\frac{M_h}{M_1})) - f(0), \tag{8}$$

where $M_1$ is the characteristic halo mass, $\epsilon$ is a fitting factor and where $f(x)$ is defined as:

$$f(x) = -log_{10}(10^{\alpha x}+1) + \delta\frac{(log_{10}(1+exp(x)))^\gamma}{1+exp(10^{-x})}, \tag{9}$$

where $\alpha$ is the low-mass power slope, $\gamma$ is a fitting index and $\delta$ is a fitting factor.

We use the FMR prescribed by Heintz et al. (2021):

$$\tilde{Z}(M_*, {\rm SFR}) = \tilde{\rm Z}_0 - (\gamma/\beta){\rm log}(1 + ({\rm M}_*/{\rm M}_0({\rm SFR}))^{-\beta}), \tag{10}$$

where $M_0({\rm SFR}) = 10^{\rm m_0} \times {\rm SFR}^{\rm m_1}$, with best-fit parameters $\tilde{Z}_0 = 8.779$, $m_0 = 10.11$, $m_1 = 0.56$, $\gamma = 0.31$ and $\beta = 2.1$. Here, the metallicity $\tilde{Z}$ is not in units of solar metallicity. To convert, we do:

$$Z = 10^{\tilde{Z}-\tilde{Z}_0}. \tag{11}$$

This pipeline allows to calculate the metallicity of each halo from their mass. Using equation 7, we now have an ameliorated model for the modelling of the [CII] signal, which is dependent on halo HI mass and metallicity.

### 2.4. *Error Analysis*

We now are able to produce the pure [CII] signal modeled by our equation described in section 2.3. On top of the signal, we would like to generate forecasts of observational experiments. To do so, we can use the pure signal and add noise to it. This noise is defined differently depending on the observational conditions.

#### 2.4.1. *cm-wave Observations*

We perform our error analysis by adding Gaussian noise, which effectively is a sensitivity per voxel. For cm-wave observations, this sensitivity is given by:

$$\sigma_{\rm n} = \frac{\rm NET}{\sqrt{t_{\rm pix}N_{\rm feeds}}}, \tag{12}$$

where $t_{\rm pix}$ is the observation time for each detector, $N_{\rm feeds}$ is the number of instruments' feeds and NET is the instrumental noise equivalent temperature, which is given by:

$$\rm NET = \frac{T_{sys}}{\sqrt{\delta_\nu}}, \tag{13}$$

where $T_{\rm sys}$ is the system temperature and $\delta_\nu$ is the frequency increment between the different redshifts analyzed (Chung et al., 2020) **??**.

#### 2.4.2. *mm-wave Observations*

In an analog fashion, the sensitivity per voxel for mm-wave observations is given by:

$$\sigma_{\rm n} = \frac{\rm NEI}{\sqrt{t_{\rm pix}N_{\rm feeds}}}, \tag{14}$$

where NEI is the noise equivalent intensity, which is an indicator of the sensitivity per instrumental pixel per spectral element. It is defined by:

$$\rm NEI = \frac{NEFD}{\Omega_{beam}}, \tag{15}$$

where NEFD is the noise equivalent flux density (the noise per beam) and $\Omega_{\rm beam}$ is the angular area in the sky covered by the instrument (Chung et al., 2020) **??**.

From there, we can use specific values for the NEFD, $\Omega_{\rm beam}$, $t_{\rm pix}$, $N_{\rm feeds}$ and $\delta_\nu$ to implement our error. Here we perform CCAT prime forecasts, so we use values of NEFD = 72.5 mJy s$^{1/2}$, $\Omega_{\rm beam}$ = 4 deg$^2$, $t_{\rm pix}$ = 0.016h [corresponds to $t_{obs}$ = 2000h], $N_{\rm feeds}$ = 120 and $\delta_\nu$ = 2.8 GHz (CCAT-prime Collaboration, 2022) **??**.

### 2.5. *Making the Map*

Now that we are able to produce the pure [CII] signal and to model the noise corresponding to specified observational conditions, we can make forecast maps for the observation of [CII] luminosity lines.

First, the luminosity lines of each halo is being computed through the model described in section 2.3. Then, the `limlam_mocker` code takes care of producing the map objects with the dimensional specifications from our parameters. Along that, it bins the [CII] luminosities in 3D data cubes for the map. Combining the two allows to generate the full data cube of [CII] luminosities. We can then look at a slice of that cube (whether that be at a specific redshift, RA or DEC).

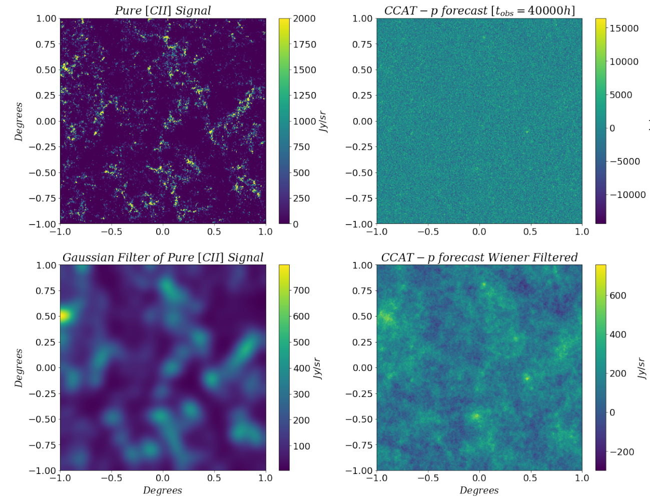


FIG. 1.— Left panels: Pure [CII] signal maps (bottom one is Gaussian filtered). Right panels: [CII] forecast maps for CCAT-prime (bottom one is Wiener filtered).

## 3. SUPERVISORSHIP

This line intensity mapping research work, which is being developed over this summer 2022 at the Canadian Institute for Theoretical Astrophysics, is being supervised by Prof. Dick Dond and Dr. Dongwoo Chung under a Summer Undergraduate Research Fellowship (SURF).

REFERENCES

[1] Tony Y. Li, Risa H. Wechsler, Kiruthika Devaraj, and Sarah E. Church. CONNECTING CO INTENSITY MAPPING TO MOLECULAR GAS AND STAR FORMATION IN THE EPOCH OF GALAXY ASSEMBLY. *The Astrophysical Journal*, 817(2):169, jan 2016.